Biochemical Pharmacology 136 (2017) 136–149

Contents lists available at ScienceDirect

Biochemical Pharmacology

journal homepage: www.elsevier.com/locate/biochempharm

Apigenin, a modulator of PPARγ, attenuates HFD-induced NAFLD by regulating hepatocyte lipid metabolism and oxidative stress via Nrf2 activation

Xiujing Feng [a], Wen Yu [a], Xinda Li [a], Feifei Zhou [a], Wenlong Zhang [a], Qi Shen [b], Jianxin Li [b], Can Zhang [c,d,*], Pingping Shen [a,*]

[a] State Key Laboratory of Pharmaceutical Biotechnology and MOE Key Laboratory of Model Animal for Disease Study, Model Animal Research Center, Nanjing University, Nanjing 210023, China
[b] Key Lab of Analytical Chemistry for Life Science, School of Chemistry and Chemical Engineering, Nanjing University, Nanjing 210023, China
[c] State Key Laboratory of Pharmaceutical Biotechnology, Nanjing University, Nanjing 210023, China
[d] Center of Drug Discovery, State Key Laboratory of Natural Medicines, China Pharmaceutical University, Nanjing 210009, China

ARTICLE INFO

Article history:
Received 7 February 2017
Accepted 12 April 2017
Available online 13 April 2017

Keywords:
Apigenin
NAFLD
Nrf2
PPARγ

ABSTRACT

Lipid metabolic disorders and oxidative stress in the liver are key steps in the progression of nonalcoholic fatty liver disease (NAFLD), which is a major risk factor for the development of metabolic syndrome. To date, no pharmacological treatment for this condition has been approved. Our previous study has found that the food-derived compound apigenin (Api) significantly attenuates obesity-induced metabolic syndrome by acting as a peroxisome proliferator-activated receptor gamma modulator (PPARM). Herein, a high fat diet (HFD) induced NAFLD model was used to dig out whether Api had the effect on NAFLD. The results showed that Api had obvious effect in restraining NAFLD progression, including attenuating HFD induced lipid accumulation and oxidative stress *in vivo*. As a PPARM, although Api did significantly inhibit the expression of PPARγ target genes encoding the protein associated with lipid metabolism, it had no obvious activating effect on PPARγ. Interestingly, we found that Api promoted Nrf2 into the nucleus, thereby markedly activating Nrf2 to inhibit the lipid metabolism related genes and increase the oxidative stress related genes. Further Nrf2 knockdown/knockout and overexpression experiments showed that Api regulating PPARγ target genes was dependent on Nrf2 activation and the activation of Nrf2 counteracted the activation effect of PPARγ by Api. Importantly, we also found that Api might bind with Nrf2 via auto dock and ITC assay. Therefore, our results indicate that Api ameliorates NAFLD by a novel regulating mode of Nrf2 and PPARγ in inhibiting lipid metabolism and oxidative stress abnormity.

1. Introduction

Nonalcoholic fatty liver disease (NAFLD), characterized by excessive triglyceride (TG) and oxidative stress in the liver [1], is the hepatic manifestation of metabolic syndrome. It encompasses a disease spectrum from simple steatosis (TG accumulation in hepatocytes) to nonalcoholic steatohepatitis (NASH), fibrosis, irreversible cirrhosis and even hepatocellular carcinoma [2] and has been recognized as the leading cause of chronic liver disease. The pathogenesis of NAFLD appears to involve a multiple-hit process, such as the development of macrovesicular steatosis and oxidative stress from mitochondrial reactive oxygen species (ROS). To date, there are no effective medical interventions that can completely reverse the disease other than lifestyle changes, dietary alterations and, possibly, bariatric surgery [3]. Available treatments with demonstrated benefits include the antioxidant vitamin E, the insulin-sensitizing agent pioglitazone [4], and obeticholic acid; however, the effect sizes are modest (<50%), and none of these treatments have been approved by the US Food and Drug Administration [5]. A major challenge to drug efficacy in general is that drugs are intended to act on a single target in the pathology of a disease [6]. Thus, identifying drugs or compounds that can simultaneously regulate different proteins might effectively curb the progression of NAFLD.

* Corresponding authors.
E-mail addresses: zhangcan@cpu.edu.cn (C. Zhang), ppshen@nju.edu.cn (P. Shen).

http://dx.doi.org/10.1016/j.bcp.2017.04.014
0006-2952/

Natural products extracted from medical plants are rich sources of biologically active substances and have desirable health benefits and effects on the prevention of human diseases. Recently, increasing numbers of studies have focused on herbal extracts or natural products with anti-hyperlipidemia and hepato-protective effects against NAFLD [7]. Flavonoids constitute the largest class of dietary phytochemicals, adding essential health value to the diet, and they are emerging as key nutraceuticals [8]. These phytochemicals have positive effects on lipid metabolism [9], insulin resistance [10] and oxidative stress [11], which are the most important pathophysiological pathways in NAFLD. Among these, Api (4,5,7-trihydroxyavone), a naturally occurring flavonoid present in a variety of fruits and leafy vegetables, has many pharmacological activities, such as antioxidant [12] and anti-cancer [13]. In addition, Api also can protect against HFD-induced hepatosteatosis in rats [7] and prevent lipid peroxidation, thereby having hepato-protective effects [14]. Moreover, NAFLD is a major risk factor for the development of metabolic syndrome and our recently research has found that Api is a PPARM that inhibits obesity-induced metabolic syndrome via binding and activating PPARγ [15]. Hence, further study of Api and the potential mechanism related to improving NAFLD has potential therapeutic implications.

Nrf2, a target for new therapeutic approaches aimed at treating liver diseases [16,17], has been well established as a master regulator of lipid metabolism homeostasis and oxidative stress [18]. Additionally, it is well known that the actin-bound protein Kelch-like ECH-associated protein 1(Keap1) interacts with Nrf2 and forms a complex to repress the function of Nrf2 [19]. Inducers disrupt the cytoplasmic complex, thereby releasing Nrf2 to migrate to the nucleus where it activates the antioxidant response element (ARE) of phase 2 genes and promotes the activation of its target genes. Nrf2 positively regulates the expression of anti-oxidant genes and phage II metabolizing enzymes and negatively regulates hepatosteatosis genes. Moreover, Nrf2 has garnered attention in nutrition-related liver diseases. Feeding mice diets containing ethanol [20] or a high concentration of fat [18] results in more severe liver injuries in Nrf2-null mice than in wild-type mice. In particular, the endogenous mRNA and protein levels of Nrf2 and Nrf2 target genes, such as heme oxygenase-1 (HO-1), were significantly increased by Api, thereby protecting against oxidative stress [21,22]. It is worth noting that PPARγ is one of Api's therapeutic targets in human disease [8]. PPARγ, as a ligand-dependent transcription factor, plays central roles in lipid metabolism and oxidative stress. Generally, it is increased in fatty liver disease associated with obesity in both mouse models [23] and humans [24]. Hepatocyte/macrophage-specific PPARγ knockout protects against hepatic steatosis, and PPARγ knockdown by RNA interfering-adenoviral vector injection improves fatty liver in high-fat diet (HFD)-fed mice [25,26]. In addition, the treatment of ob/ob mice with rosiglitazone (Rosi) (the classical agonist of PPARγ) does not reverse histological NAFLD but instead increases oxidative stress and liver steatosis [27]. However, treatment with thiazolidinedione improves hepatic steatosis and protection from NASH and hepatic fibrosis via increasing insulin sensitivity in adipose tissue and skeletal muscle, overcoming the direct steatogenic effect in hepatocytes [28,29]. Previous studies suggested that the role of PPARγ in fatty liver may be due to the state of microenvironment and its actions on different tissues and pathways. Thus, we focused on a PPARM Api [15,30,31], in improving HFD-induced liver lipid metabolic disorders and oxidative stress via acting on the hepatocytes. In the current study, we found that Api significantly inhibited the progression of NAFLD. Importantly, Api activated Nrf2 by promoting Nrf2 translocation into the nucleus. Further study indicated that Nrf2 activation by Api inhibited the function of Api activating PPARγ, thereby leading to the inhibition of NAFLD progression.

2. Methods

2.1. Chemicals, reagents, antibodies and plasmids

Api, PubChem CID: 5280443, purity > 99%, purchased from Zelang biotechnology company (Nanjing, China). Rosi (PubChem CID: 77999), sulforaphane (SFN) (PubChem CID: 24724610), Sodium oleate (PubChem CID: 24898044) and Methyl Palmitate (PubChem CID: 24898607) were purchased from Sigma (St. Louis, MO) (see Table 1). Dulbecco's modified Eagle's media (DMEM) and fetal bovine serum (FBS) were purchased from Gibco (Grand Island, NY). Oil red, radio immunoprecipitation assay (RIPA) lysis buffer, the nucleus protein and cell plasma protein extraction kit (P0028) and MTT are from Beyotime (Haimen, Jiangsu, China). Superoxide dismutase (SOD) assay kit (A001-3), glutathione peroxidase (GSH-Px) assay kit (A005), total glutathione/oxidized glutathione assay kit (A061-2), catalase (CAT) assay kit (Visible light) (A007-1), protein carbonyl assay kit (A087), TG assay kit (F001-1) and methane dicarboxylic aldehyde (MDA) assay kit (TBA method) (A003-1) were bought from Jiancheng biology institution (Nanjing, Jiangsu, China). Lipofectamine™ 2000 was purchased from Invitrogen (Carlsbad, CA). NEB buffer 2 (B7002S), NEB buffer 3.1(B7203S), BsmBI (R0580S), T4 ligation buffer (B0202S), T4 DNA ligase (M0202S), T7 endonuclease I (M0302S) were bought from NEW ENGLAND BioLabS. PPARγ antibody (sc7273) and Keap1 antibody (sc15246) were purchased from Santa Cruz Biotechnology, Santa Cruz, CA. Nrf2 antibody (BS6286) and Lamin A/C (R386) pAb were purchased from Bioworld technology company (Nanjing, China). HRP-conjugated GAPDH was bought from Kangchen (Shanghai, China). HRP-conjugated goat anti-rabbit IgG (H + L) and HRP-conjugated goat anti-mouse IgG (H + L) were from Beyotime (Haimen, Jiangsu, China). ARE-Luc plasmid, PPRE-Luc plasmid and dual-luciferase reporter assay system were from Promega (Madison, WI, USA). Nrf2-shRNAs were purchased from Gene biology institution (Shanghai, China). LentiCRISPRv2 was from the Prof Cui (Sun Yat-Sen University).

2.2. Mice and treatment

Male C57BL/6J mice (3–4 weeks old) were purchased from Animal Genetics Research Center of Nanjing University (Nanjing, China) and housed in specific-pathogen-free (SPF) facility. Mice, starting at age of 3–4 weeks old, were randomly divided into four groups ($n = 9$ per group). Mice were fed for 16 weeks either on a normal chow diet (ND) consisting of 4.5% fat or a HFD (D12492, 60% fat, 20% carbohydrate, 20% protein, total 5.24 kcal/g; Research Diets Inc., New Brunswick, NJ). 19-week -old mice were grouped and injected with Api (30 mg/kg), Rosi (10 mg/kg) or vehicle alone (saline containing 0.1% DMSO) intraperitoneally daily for 3 weeks. Mice were weighed daily until sacrificed under anesthesia using diethylether. Animal welfare and experimental procedures were followed in accordance with the Guide for Care and Use of Laboratory Animals (National Institutes of Health, the United States) and the related ethical regulations of Nanjing University.

2.3. Hematoxylin and eosin (H&E)

After the mice were sacrificed, the livers were removed and subsequently fixed in phosphate-buffered 10% formalin, and embedded in paraffin blocks. A section from each paraffin block was stained with hematoxylin and eosin to examine the pathologic structures of the tissues and to score the liver steatosis for five to eight sections/400 × field, five to six fields/gland/mouse, score according to the grade of lesion, slight (0.5), mild (1), moder-

ate (2), severe (3), profound severe (4) and normal (0), (n = 6). Images were obtained from fluorescence microscopy.

2.4. Biochemical analyses

The liver tissues stored in the deep freezer were removed on the day of analysis and weighed. The tissues were washed with cold physiological saline and the tissues were cut into small pieces with scissors and transferred into glass tubes for homogenization. After stirring, some of the homogenate was transferred into Eppendorf tubes for GSH and MDA measurements. The homogenate was centrifuged at 3000 rpm for 10 min and the supernatants obtained were used to measure the activities of SOD, GSH-Px and CAT. Additionally, the supernatants were sonificated three times for 10 s to measure the CAT enzyme activity. Protein content was also measured in the supernatant in which enzymatic activities were measured. Analyses of carbonylated proteins were performed using protein carbonyl assay kit. Briefly, 100 μL of protein samples were mixed with 400 μL of 10 mM 2, 4-dinitrophenyl hydrazine (DNPH) (in 2 M HCl) and incubated for 30 min at room temperature. Proteins were precipitated with equal volume of 30% TCA, and the pellets were washed three times with 1 mL ethanol-ethyl acetate (1:1, v/v). The pellets were dissolved in 1.25 mL of 6 M guanidine HCl and kept at 37 °C for 15 min. The carbonyl content was calculated from the absorbance at 370 nm using a molar absorption.

2.5. Cell culture and drug treatment

Murine hepatoma Hepa1-6 cell line was obtained from Shanghai Institutes for Biological Sciences, Chinese Academy of Sciences (Shanghai, China). The cells were grown as a monolayer culture in DMEM supplemented with 10% FBS, 100 U/mL penicillin, 100 g/mL streptomycin, in monolayer culture, and were incubated at 37 °C in a humidified atmosphere containing 5% CO_2 in air. The cell model of NAFLD was developed as previously described [32,33]. Briefly, Hepa1-6 cells (1×10^4/mL) were plated into a 48-well plate containing 100 μL of cell culture medium. When ~80% confluence was reached and cells were cultured in FBS-free medium for 24 h, then cells were treated with or without 0.5 mM or 1 mM long-chain FFA (2:1 oleate/palmitate, Sigma, St. Louis, MO) in media containing 1% bovine serum albumin to develop a steatosis model, which was assayed by oil red staining.

2.6. Cell viability assay

1×10^4 Hepa1-6 cells were seeded in 96-well plates, and the next day (at ~80% confluence) cells were treated with various concentrations (0.2–64 μM) of Api for 24 h, in a set of three replicates including control (0.1% DMSO). Adherent cells were assayed by MTT assay.

2.7. Western blot

Cell/tissue samples for were lysed with RIPA containing freshly added protease inhibitor tablets (Roche Applied Science, Mannheim, Germany) and the nucleus protein and cytoplasmic protein were extracted according to the nucleus protein and cell plasma protein extraction kit's instruction. The protein concentrations were determined using a BCA kit (Beyotime, Haimen, Jiangsu, China). The whole cell/tissue lysates were subjected to reducing 10% SDS-polyacrylamide gel electrophoresis (PAGE), transferred onto PVDF membranes (Millipore, Bedford, MA, USA), blocked with 5% bull serum Albumin for 2 h at room temperature, and immunoblotted at 4 °C overnight with the primary antibody for Nrf2 (dilution 1:1000), Keap1(1.:1000) or PPARγ (dilution 1:200). The blots were visualized using an enhanced chemiluminescent method kit (Cell Signaling Technology, Danvers, MA, USA). As an internal control for equal protein loading, blots were stripped and probed with antibodies against GAPDH or Lamin A/C. The band intensity analysis of western blotting was performed using the Image J software.

2.8. Luciferase assay

Cells were seeded in 48-well cell culture plates in triplicate and allowed to grow overnight to reach ~80% confluence. Then the cells were transfected with plenti-Nrf2/ARE-Luc and PRL-control or with pIRES-mPPARγ/PPRE-Luc and pRL-control (containing *Renilla* luciferase cDNA) using Lipofectamine 2000 transfection reagent. After 24 h, luciferase activities were measured using the dual-luciferase reporter assay system. *Renilla* luciferase activity was normalized to firefly luciferase activity.

2.9. CRISPR-CAS9-Nrf2 knockout in hepatocyte

Constitutive exons near the 5′ end of transcripts are identified using NCBI CCDS datasets. The gRNA targeting Nrf2 genes were designed by online tool developed by Prof Zhang (http://crispr.mit.edu/). gRNA were ranked by an off target score using a metric that includes the number of off-target in the genome and the type of mutations (distance from protospacer-adjacent motif and clustering of mismatches) and those with lowest off-target scores were selected. Thus, gRNA designed to target the common exons for all mouse Nrf2 isoforms were synthesized as follows: gRNA1-5′-CACCGGAGTAGC TGGCGGATCCAC-3′, gRNA2-5′-AAACGTG GATCCGCCAGCTA CTCC-3′, and cloned to PlentiCRISPRv2 (one vector system, lined by BsmBI) plasmids [34]. Then viral vector were produced in HEK293T cells and concentrated to increase viral titer. After the plasmids were transfected into Hepa1-6 cells for 24 h, cells were selected with 2 μg/mL puromycin for 48 h. The cells were trypsinized and seeded into 96-well plates. Then the genome DNA extracted from all of the clones was tested by cloning PCR using primer M-Nrf2-seqF and M-Nrf2-seqR. Then the T7E1 enzyme was and DNA sequencing were used to find the positive cells transduced with a lentiCRISPR construct preserved. Finally, the western blotting was used to detect the complete deletion of the gene.

2.10. Quantitative real-time PCR (qRT-PCR)

Total RNA was extracted from tissues or cells and reverse-transcribed to cDNA using BioTeke supermoIII RT Kit (Bioteke Corporation, Beijing, China). The mRNA expression of mouse Nrf2, mouse PPARγ, the oxidative stress relative genes such as Gclc, Gclm, Gsta2, Gsta4, Gstm1 and Nqo1, the Lipid droplet formation genes including Cidea, Fitm1, Fitm2, Plin2, G0s2, the lipid uptake genes Lpl, Fabp1, Fatty acid oxidation genes including mCPT-1, PDK4, ACOX1, ACAA2 and the lipogenesis genes Fasn, SCD1, HMGCR, ACACA and Nrob2 were detected by qRT-PCR, which was performed with the iCycler thermocycler system and iQ5 optical system (Bio-Rad) using SYBR green I dye (Bio-Rad). The studied gene names were listed in Table 2. Threshold cycle numbers were obtained using iCycler thermocycler system software version 10 PCR cycling conditions were as follows: 1 cycle of 94 °C for 5 min followed by 40 cycles of 94 °C for 30 s, 60 °C for 30 s, and 72 °C for 45 s. The primers used were listed in Table 3. Relative mRNA expression of target genes was obtained by normalizing to control group and the level of β-actin, by using $2^{-\Delta\Delta Ct}$ method [35].

Table 1
The compound used in this paper.

Name	PubChem CID
Apigenin (Api)	5280443
Rosiglitazone (Rosi)	77999
Sulforaphane (SFN)	24724610
Sodium oleate	24898044
Methyl Palmitate	24898607

2.11. Expression of recombinant Nrf2-his

The cDNA coding sequence for the Nrf2 protein including SacI/Xbal was amplified by PCR, and then inserted into a pCzn1 plasmid in frame to the C-terminal of 6 × His tag. The inserted Nrf2 in pCzn1-Nrf2 was sequenced. Nrf2-his was expressed in Arctic Express™ transformed with the pCzn1-Nrf2 expression plasmid. A culture was grown in Luria–Bertani (LB) medium containing 50 μg/ml ampicillin at 37 °C until the OD600 nm was 0.6–0.8, at which point isopropyl-β-D-thiogalactopyranoside (IPTG) (0.5 mM, final) was added to induce protein expression.

2.12. Purification of recombinant Nrf2-his

Cells were harvested 12 h later and resuspended in Lysis buffer containing 20 mM Tris-HCl, 1 mM phenylmethylsulfonyl fluoride (PMSF) and bacteria protease inhibitor cocktail (pH8.0), then sonicated 100 times for 12 s. Samples were centrifuged for 20 min at 10×10^3 g and 4 °C. Precipitated material (inclusion bodies) containing Nrf2-his was washed three more times by resuspending the material in 20 mM Tris, 1 mM EDTA, 2 M Urea, 1 M NaCl, 1% Triton X-100 (pH8.0), followed by centrifugation. Pellets from the final wash were resuspended in buffer A [20 mM Tris (pH7.9), 5 mM DTT and 8 M Urea] and protein was extracted by overnight nutation at 4 °C. After centrifugation to remove the remaining insoluble material, samples containing Nrf2-his were aliquoted and stored at −80 °C. Nrf2-his can be further purified by dialysis and Ni-NTA–agarose affinity chromatography. The purification was identified by Coomassie Brilliant Blue staining.

Table 2
List of the studied gene names.

Gene names	Gene aliases
Nrf2	NF-E2-related factor 2
PPARγ	Peroxisome proliferator-activated receptor gamma
Gclc	Glutamate cysteine ligase catalytic subunit
Gclm	Glutamate cysteine ligase modifier subunit
Gsta2	Glutathione S-transferase class Alpha2
Gsta4	Glutathione S-transferase class Alpha4
Gstm1	Glutathione S-transferase M1
Cidea	Cell death-inducing DNA fragmentation factor-α-like effector A
Plin2	Perilipin 2
Lpl	Lipoprotein lipase
Nr0b2	SHP, small heterodimer partner
Fitm1	Fat-induced transcript 1, FIT1
Fitm2	Fat-induced transcript 2, FIT2
G0s2	G0/G1 switch gene 2
Fabp1	Fatty acid binding protein-1 genes
Nqo1	NAD (P) H: quinone oxidoreductase 1
PPARα	Peroxisome proliferator-activated receptor α
Srebf1	Sterol regulatory element binding protein-1
Elovl2	Elongation of very long-chain fatty acids 2
Lipc	Hepatic lipase
PLA2G7	Platelet-activating factor acetylhydrolase
Fasn	Fatty acid synthase
mCPT	Muscle carnitine palmitoyltransferase I
PDK4	Pyruvate dehydrogenase kinase 4
ACOX1	Acyl-CoA oxidase 1
Hmgcr	3-hydroxy-3-methylglutaryl coenzyme A
Hmgcs2	Hydroxymethylglutaryl CoA synthase 2
SCD1	Stearoyl-CoA desaturase–1
SOD1	Superoxide dismutase 1
Acaa2	Acetyl-coenzyme A acyltransferase 2
Gsr	Glutathione reductase
Acaca	Acetyl-CoA carboxylase alpha

Table 3
Primers used in this paper.

Nrf2(qPCR)-F	5′-CAG CAC ATC CAG TCA GAA ACC-3′
Nrf2(qPCR)-R	5′-AGC CGA AGA AAC CTC ATT GTC-3
NQO1-F	5′-AGC GTT CGG TAT TAC GAT CC-3′
NQO1-R	5′-AGT ACA ATC AGG GCT CTT CTC G-3′
GCLm-F	5′-TGA CTC ACA ATG ACC CGA AA-3′
GCLm-R	5′-CTT CAC GAT GAC CGA GTA CCT-3′
GSTM1-F	5′-GCA GCT CAT CAT GCT CTG TT-3′
GSTM1-R	5′-CAT TTT CTC AGG GAT GGT CTT C-3′
GSTA2-F	5′-TCT GAC CCC TTT CCC TCT G-3′
GSTA2-R	5′-GCT GCC AGG ATG TAG GAA CT-3′
GSTA4-F	5′-TCC GAC TTC CCT CTG CTG-3′
GSTA4-R	5′-AAC ATA GGG GCC ATC TGG A-3′
GCLc-F	5′-AGA TGA TAG AAC ACG GGA GGA G-3′
GCLc-R	5′-TGA TCC TAA AGC GAT TGT TCT TC-3′
Fabp1-F	5′-ATG AAC TTC TCC GGC AAG TAC C-3′
Fabp1-R	5′-CTG ACA CCC CCT TGA TGT CC-3′
LPL-F	5′-GGG AGT TTG GCT CCA GAG TTT-3′
LPL-R	5′-TGT GTC TTC AGG GGT CCT TAG-3′
Nrob2-F	5′-TGG GTC CCA AGG AGT ATG C-3′
Nrob2-R	5′-GCT CCA AGA CTT CAC ACA GTG-3′
Cidea-F	5′-TGA CAT TCA TGG GAT TGC AGA C-3′
Cidea-R	5′-GGC CAG TTG TGA TGA CTA AGA C-3′
Plin2-F	5′-GAC CTT GTG TCC TCC GCT TAT-3′
Plin2-R	5′-CAA CCG CAA TTT GTG GCT C-3′
Fitm1-F	5′-CCT CTG CCT TAC TGT ACT TTG G-3′
Fitm1-R	5′-TAG CGA AGA TCG TCC GAG AGT-3′
Fitm2-F	5′-TCG GTC GTC AAG GAG CTG T-3′
Fitm2-R	5′-GAG GAC GTT GCG CTT GTT G-3′
G0s2-F	5′-TAG TGA AGC TAT ACG TTC TGG GC-3′
G0s2-R	5′-GTC TCA ACT AGG CCG AGC A-3′
Srebf1-F	5′-GAT GTG CGA ACT GGA CAC AG-3′
Srebf1-R	5′-CAT AGG GGG CGT CAA ACA G-3′
Elovl2-F	5′-CCT GCT CTC GAT ATG GCT GG-3′
Elovl2-R	5′-AAG AAG TGT GAT TGC GAG GTT AT-3′
Lipc-F	5′-ATG GGA AAT CCC CTC CAA ATC T-3′
Lipc-R	5′-GTG CTG AGG TCT GAG ACG A-3′
PLA2G7-F	5′-CTT TTC ACT GGC AAG ACA CAT CT-3′
PLA2G7-R	5′-CGA CGG GGT ACG ATC CAT TTC-3′
PPARγ-F	5′-GGA AGA CCA CTC GCA TTC CTT-3′
PPARγ-R	5′-TCG CAC TTT GGT ATT CTT GGA G-3′
β-Actin-F	5′-GCT CTG GCT CCT AGC ACC-3′
β-Actin-R	5′-CCA CTA TCC ACA CAG AGT ACT TG-3′
mCPT-1-F	5′-GAG GAC AGA TGT GGT GGG TTT-3′
mCPT-1-R	5′ AGG AGT CAA CTC AGC TTT CTC TT-3′
PDK4-F	5′-AGG GAG GTC GAG CTG TTC TC-3′
PDK4-R	5′-GGA GTG TTC ACT AAG CGG TCA-3′
ACOX1-F	5′-TAA CTT CCT CAC TCG AAG CCA-3′
ACOX1-R	5′-AGT TCC ATG ACC CAT CTC TGT C-3′
Fasn-F	5′-GGA GGT GGT GAT AGC CGG TAT-3′
Fasn-R	5′-TGG GTA ATC CAT AGA GCC CAG-3′
Hmgcr-F	5′-AGC TTG CCC GAA TTG TAT GTG-3′
Hmgcr-R	5′-TCT GTT GTG AAC CAT GTG ACT TC-3′
Hmgcs2-F	5′-GAA GAG AGC GAT GCA GGA AAC-3′
Hmgcs2-R	5′-GTC CAC ATA TTG GGC TGG AAA-3′
SCD1-F	5′-TTC TTG CGA TAC ACT CTG GTG C-3′
SCD1-R	5′-CGG GAT TGA ATG TTC TTG TCG T-3′
SOD1-F	5′-AAC CAG TTG TGT TGT CAG GAC-3′
SOD1-R	5′-CCA CCA TGT TTC TTA GAG TGA GG-3′
Gaps-F	5′-TCC TCA GGT CAA GCA AGT GTT-3′
Gaps-R	5′-TGG TCC GAC AAC TAC GAG TTC-3′
Acaa2-F	5′-CTG CTA CGA GGT GTG TTC ATC-3′
Acaa2-R	5′-AGC TCT GCA TGA CAT TGC CC-3′
GSR-F	5′-GAC ACC TCT TCC TTC GAC TAC C-3′
GSR-R	5′-CCC AGC TTG TGA CTC TCC AC-3′
ACACA-F	5′-GAT GAA CCA TCT CCG TTG GC-3′
ACACA-R	5′-GAC CCA ATT ATG AAT CGG GAG TG-3′
M-Nrf2-seqF	5′-GCT ATT TCT GTT GTT TTG CAG TC-3′
M-Nrf2-seqR	5′-ACT TCT CCT CCT CAC AAA AGA C-3′

2.13. Isothermal titration calorimetry (ITC)

ITC experiments on the alpha subtype were performed at 25 °C using a MicroCal ITC200 microcalorimeter (MicroCal Inc., Northampton, MA, USA). Protein was extensively dissolved in a buffer of PBS (pH 7.4) and the PBS buffer was used to dilute the Api stock solutions (185 mM in DMSO). DMSO was added to the protein solution in the same percentage of the ligand solution (below 0.05%). Protein solution (50 μM) was added to the sample cell and the ligand solution (10 times more concentrated than the protein) was injected into the cell in 19 aliquots of 20 μl for 4 s (the first injection was 0.4 μl for 0.8 s) with delay intervals between injections of 120 s. Reference titration of ligand into buffer was used to correct for heat of dilution. The syringe stirring speed was set at 1000 rpm. The thermodynamic data were processed with Origin 7.0 software provided by MicroCal. To correct for any discrepancies in the baseline outlined by the software, a manual adjustment was performed.

2.14. Statistical analysis

The data were expressed as the mean ± standard error of mean (SEM). The statistical analysis was performed by the Student *t*-test when only two value sets were compared. A one-way ANOVA followed by a Dunnett's test was used when the data involved three or more groups, as indicated in the Figure legends. All of the statistical tests and graphical presentation were performed using the Prism 5.0 software (GraphPad, San Diego, CA). $P < 0.05$, $P < 0.01$ or $P < 0.001$ were considered statistically significant and indicated by *, ** or ***, respectively.

3. Results

3.1. Api attenuates HFD-induced NAFLD

Api (Fig. 1A), a food-derived compound, has been reported to have a marked attenuating effect on the steatosis of liver tissue [36]. However, the effect of Api on NAFLD progression and the potential mechanism are still unknown. To address this question, male C57BL/6 J mice fed with HFD for 16 weeks gradually developed NAFLD [37–39] were used, with or without 30 mg/kg Api treatment. Meanwhile, 10 mg/kg Rosi was used as a positive control. As Fig. 1B-C shown that various degrees of liver steatosis and many lipid droplets of different sizes were observed in all HFD-fed mice, suggesting HFD induced the derangement of cell structures and excessive lipid droplets in hepatocytes, however, this effect was alleviated by Api treatment. In addition, the levels of TG in the liver tissue increased in HFD mice were all significantly reduced by Api treatment (Fig. 1D). Moreover, we assayed the expression of inflammatory factors MCP-1 (Fig. 1E), TNFα (Fig. 1F), F4/80 (a surface marker of macrophages) (Fig. 1G), and the results indicated that Api significantly reduced the expression of inflammatory factors, suggesting Api obviously inhibited the liver inflammation.

As shown in Fig. 1H, liver weight of ND mice was significantly increased by a HFD, which was significantly restored by Api or Rosi treatment. Meanwhile, we analyzed the liver index (liver/body weight) and found that it was also obviously reduced by Api or Rosi treatment (Fig. 1I). Additionally, NAFLD is a disease caused by "second hits" after fat accumulation and hepatic steatosis inflict the first hit. The second hits may include enhanced lipid peroxidation and oxidative stress [40]. Therefore, the levels of lipid peroxidation in the liver tissue were tested. MDA content in liver tissues of HFD mice was markedly decreased after Api or Rosi treatment (Fig. 1J). In addition, the levels of antioxidant enzyme activity are the indices of the oxidative stress response. The effect of Api treatment on HFD-induced liver oxidative stress was also detected. The results showed that Api notably increased the activities of antioxidative enzymes in liver, such as an endogenous anti-oxidase SOD (Fig. 1K), CAT (Fig. 1L) and GSH-Px (Fig. 1M), which were all obviously inhibited by a HFD. Interestingly, protein carboxylation, the most frequent and usually irreversible oxidative modification affecting proteins [41] was markedly enhanced up to 16-fold in HFD mice compared with ND mice, and Api treatment markedly decreased the effects (Fig. 1N). Carbonylated protein in the sera was also detected (Fig. 1O), and the results agreed with the data in the liver tissue. Importantly, the results of the ratio of GSH with GSSG were further indicated that Api significantly decreased liver oxidative stress (Fig. 1P). These data suggest that Api significantly attenuates HFD-induced NAFLD, including liver steatosis, fat accumulation, liver inflammation and oxidative stress of mice.

3.2. Api attenuates aberrant expression of genes affecting oxidative stress and lipid metabolism associated with NAFLD in mice

To further investigate the effect of Api on NAFLD progression, lipid metabolism-related genes, including those affecting lipid droplet formation-, lipid uptake-, lipogenesis- and oxidative stress-, were tested in the liver tissues of mice by using qRT-PCR. Lipid droplet formation-related genes, such as Cidea, Plin2, Fitm1, Fitm2 and G0s2, which were expressed at abnormally high levels in the liver tissue of HFD mice, were significantly inhibited by Api treatment (Fig. 2A). Consistently with the results for lipid droplet formation-related genes, the expression levels of lipid uptake-related genes (Fabp1 and Lpl) (Fig. 2B), the fatty oxidation genes including mCPT-1, PDK4, ACOX1, ACAA2 (Fig. 2C) and the lipogenesis-related gene Fasn, SCD1, HMGCR, ACACA and Nrob2 (Fig. 2D) in HFD mice were also markedly decreased by Api treatment. During NAFLD development, the liver tissue is under oxidative stress. Therefore, we tested the oxidative stress-related genes, such as Phase 2 enzymes, including glutathione-S-transferase (GST) isozymes, NADP(H): Quinone oxidoreductase (NQO1), heavy (catalytic) and light (modifier) subunits of glutamyl cysteine ligase (GCLc, GCLm), GSTA2 and GSTA4. As shown in Fig. 2E, the expression levels of these genes in liver were obviously decreased by HFD, but were significantly increased by Api treatment. These observations suggest that Api effectively attenuates NAFLD progression *in vivo*. In addition, Nrf2 regulates the expression of multiple cellular defense proteins through the antioxidant response element (ARE) and also functions as a major regulator of cellular lipid disposition in the liver [42]. Here, we found that Nrf2 and Keap1 were significantly enhanced in Api-treated HFD mice compared with vehicle group while the expression of PPARγ was no obvious change (Fig. 2F). Importantly, the nuclear Nrf2 level was decreased after HFD treatment but was clearly increased by Api or Rosi treatment. In contrast, the cytosolic increased Nrf2 was restored to normal levels after Api and Rosi treatment thus suggesting that Api promoted Nrf2 translocating from cytoplasm to nuclei (Fig. 2G). As to the difference that the effect of Api was more obvious than Rosi's, it might for two reasons: one is that their different binding sites with PPARγ and different capacities of activating PPARγ [36], the other might for Api not only a modulator of PPARγ but also is an antioxidant**.** Taken together with the above results, this suggests that Api can significantly inhibit the progression of NAFLD.

3.3. Api inhibits the expression of PPARγ target genes without obvious activating effect on PPARγ

In our previous study, we have indicated that Api is a PPARM and it can significantly improve obesity-induced metabolic syn-

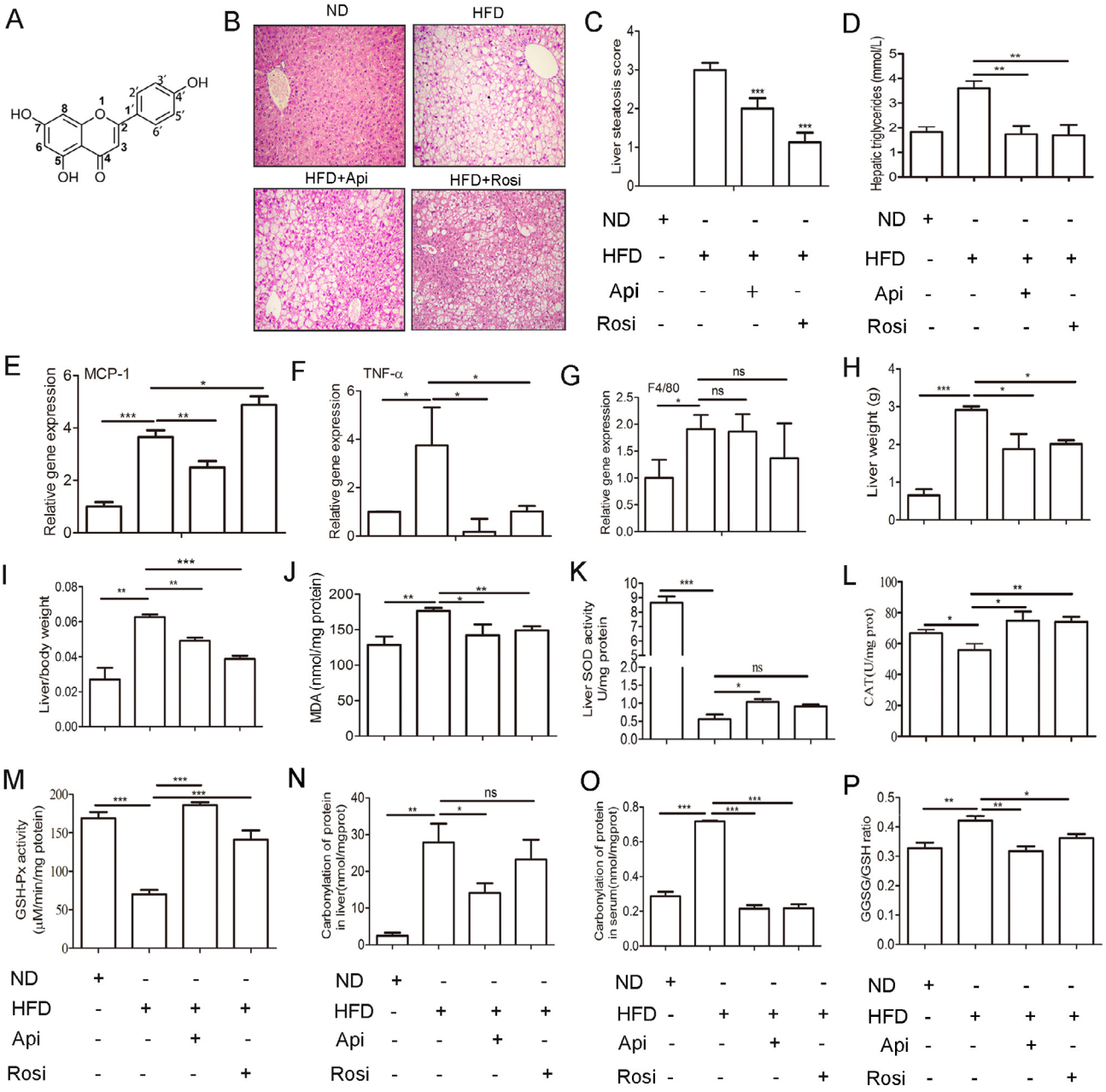

Fig. 1. Api attenuates HFD-induced NAFLD. (A) The chemical structure of Api. (B) Representative H&E staining showed liver, morphology from ND and HFD mice (n = 6) treated with the vehicle (0.1% DMSO), Api for 3 weeks, original magnification ×400 (n = 6). (C) Quantification of the steatosis of liver tissue, n = 6. (D) The TG contents in the liver tissue of ND and HFD mice (n = 6) treated with the vehicle (0.1% DMSO), Api for 3 weeks were assayed with a TG assay kit. (E-G) The inflammatory cytokine MCP-1, TNF-α, and the expression of F4/80 in the liver tissue of HFD-fed mice treated with the vehicle (0.1% DMSO), Api for 3 weeks were measured by qRT-PCR according to manufacturer's instructions (n = 6). (H) The effect of Api on mice liver weight. (I) The effect of Api on mice liver index. (J) The lipid peroxidation product MDA was tested by using a MDA assay kit. The activities of SOD (K), CAT (L), and GSH-Px (M) in the liver tissue of mice treated with vehicle (0.1% DMSO), Api (30 mg/kg) or Rosi (10 mg/kg) were measured. (N-O) The carbonyl proteins in the liver tissues/sera of mice treated with vehicle (0.1% DMSO), Api (30 mg/kg) or Rosi (10 mg/kg) were tested. (P) The ratio of GSSG/GSH in the liver tissue of mice treated with vehicle (0.1% DMSO), Api (30 mg/kg) or Rosi (10 mg/kg) were evaluated. Data are means ± SEM. Statistical analysis is based on one-way ANOVA followed by a Dunnett's test. ns, not significant, $^{*}P < 0.05$, $^{**}P < 0.01$, $^{***}P < 0.001$ *vs* ND or HFD group.

drome. To elucidate the role of PPARγ in Api attenuating NAFLD, we first established an *in vitro* model of mouse NAFLD by using different doses of free fatty acid (FFA) to stimulate mouse hepatoma Hepa1-6 for 24 h. Then, the lipid contents in the cells were analyzed by using oil red O staining and quantified on the basis of the optical density. As the Fig. 3A showed that 1 mM FFA was sufficient to induce cells to produce lipids. In addition, the effects of Api and/or FFA on the viability of hepatocytes presented in Fig. 3B showed that Api and/or FFA under the dosages we used had no significant toxicity on the viability of Hepa1-6 cells. Thus, 1 mM FFA and (1–10 μM) Api was used to perform the subsequent experiments.

Next, we investigated the role of PPARγ in Api ameliorating NAFLD. When treated with Api, the lipid accumulation was markedly decreased in the Hepa1-6 (Fig. 3C). Meanwhile, the mRNA level of PPARγ induced by FFA or HFD was significantly decreased by Api treatment (Fig. 3D). Furthermore, as shown in Fig. 3E, Api showed little effect on PPARγ activity assayed by using a luciferase reporter system while Rosi significantly enhanced PPARγ activity. However, the expression of genes targeted by PPARγ was signifi-

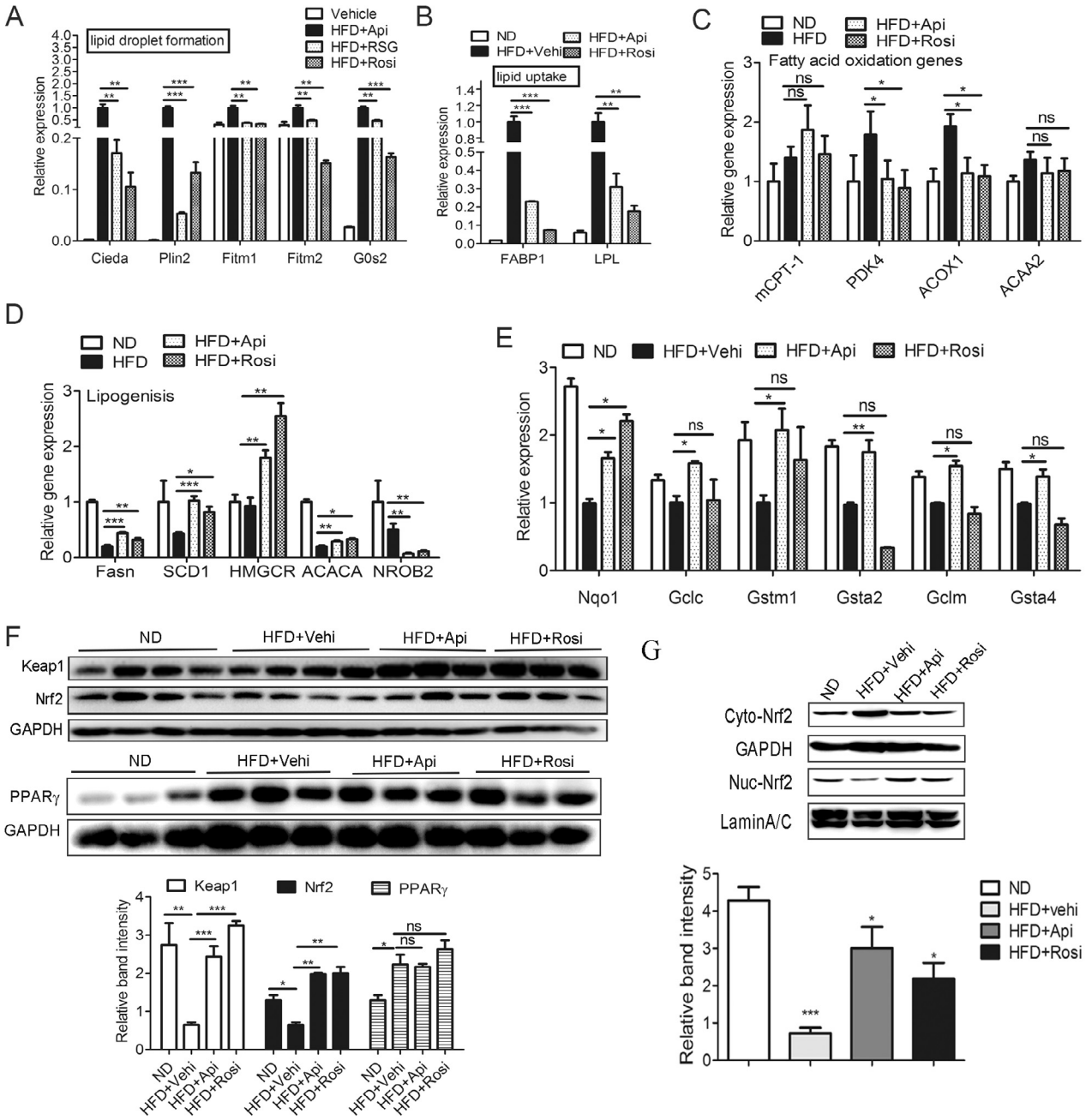

Fig. 2. Api attenuates the oxidative stress and lipid metabolism-related gene deregulation associated with NAFLD. Relative mRNA expression of lipid droplet-related genes, including Cidea, Plin2, Fitm1, Fitm2 and G0s2 (A), lipid uptake-related genes Fabp1, Lpl (B), fatty acid oxidation genes mCPT-1, PDK4, ACOX1, and ACAA2 (C), lipogenesis genes Fasn, SCD1, HMGCR, ACACA and Nrob2 (D) and oxidative stress-related genes, such as Nqo1, Gclc, Gstm1, Gsta2, Gclm and Gsta4 (E), in the liver tissues of mice treated with vehicle (0.1% DMSO), Api (30 mg/kg) or Rosi (10 mg/kg) were measured by using qRT-PCR, and normalized to (HFD + vehicle) group and β-actin level. (F) Nrf2, Keap1 and PPARγ protein expression in the liver tissues of mice treated with vehicle (0.1% DMSO), Api (30 mg/kg) or Rosi (10 mg/kg) were assayed by using western blotting and quantified by using Image J software. (G) Nuclear protein and cytoplasmic proteins were recovered from lysed liver tissue of mice treated with vehicle (0.1% DMSO), Api (30 mg/kg) or Rosi (10 mg/kg), and were subjected to western blotting and quantified by using Image J software. Data are means ± SEM. Statistical analysis is based on one-way ANOVA followed by a Dunnett's test. ns, not significant, $^{*}P < 0.05$, $^{**}P < 0.01$, $^{***}P < 0.001$ *vs* the (HFD + Vehicle) group.

cantly decreased by Api *in vitro* (Fig. 3F), which is consistent with the results obtained in obese mice (Fig. 2A). Together, these findings indicate that Api inhibits the expression of PPARγ target genes but shows no significant effect on PPARγ activity in mouse cell model of NAFLD.

3.4. Nrf2 is necessary for Api inhibiting NAFLD progression

Numerous studies have established that Nrf2 is involved in NAFLD progression [43,44]. In addition, Api, as a natural plant flavonoid, has been reported to induce dissociation of Keap1/Nrf2 complex and activation Nrf2 [45]. Also there is study indicated that Api can demethylase Nrf2 in the promoter region [46]. Our *in vivo* data also indicated that Api significantly increased Nrf2 expression in the liver tissue of HFD mice and promoted Nrf2 protein translocating into nuclei (Fig. 2F-G). Here, further studies were performed to investigate the role of Nrf2 in Api regulating NAFLD. SFN, which interacts directly with Keap1 disrupts the complex between keap1 and Nrf2, releasing Nrf2 to migrate to the nucleus, as a positive control. Firstly, the mRNA levels of Nrf2 were comparable between

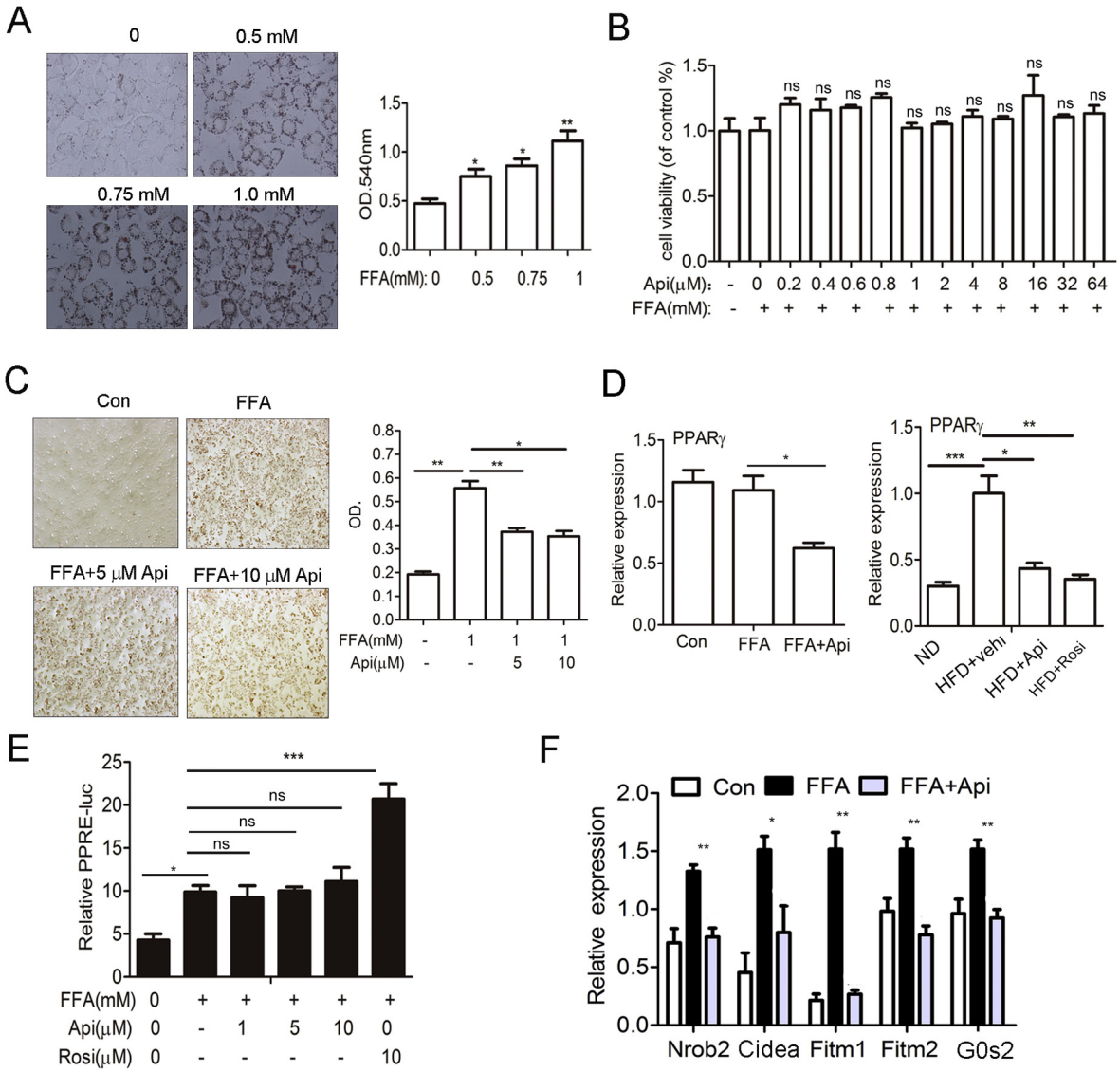

Fig. 3. Api inhibits the expression of genes targeted by PPARγ without obvious effect on PPARγ activity. (A) Hepa1-6 cells were treated with different doses of FFA (0.5–1 mM) for 12 h to establish a NAFLD cell model. Lipid accumulation was visualized using oil Red O staining (left) and then quantified according to the OD value (right). Original magnification, ×200. Data are means ± SEM. Statistical analysis is based on one-way ANOVA followed by a Dunnett's test. $^{*}P < 0.05$, $^{**}P < 0.01$ *vs* untreated group. (B) The effects of various concentrations of Api (0.2–64 μM) on the viability of Hepa1-6 cells were assayed by using the MTT method. Data are means ± SEM. Statistical analysis is based on one-way ANOVA followed by a Dunnett's test. ns, not significant *vs* FFA treated group (C) The effect of Api on FFA-induced lipid accumulation in Hepa1-6 cells was assayed by using oil Red O staining (left) and quantified on the basis of OD values (right). Original magnification, ×100. Data are means ± SEM. Statistical analysis is based on one-way ANOVA followed by a Dunnett's test. $^{*}P < 0.05$, $^{**}P < 0.01$ *vs* untreated group or FFA treated group. (D) PPARγ mRNA expression in Hepa1-6 cells or liver tissue derived from HFD mice treated with vehicle (0.1%DMSO), Api (30 mg/kg) or Rosi (10 mg/kg) was measured by using qRT-PCR and normalized to β-actin levels. Data are means ± SEM. Statistical analysis is based on one-way ANOVA followed by a Dunnett's test. $^{*}P < 0.05$, $^{**}P < 0.01$ *vs* FFA treated group or (HFD + Vehicle) group. (E) Transcriptional activation of PPARγ in cells treated with Api. Hepa1-6 cells were transfected with pIRES-mPPARγ/PPRE-Luc and pRL-control using Lipofectamine 2000. Then, cells were pre-treated with 1 mM FFA for 12 h before Api treatment for 24 h. Luciferase activities were measured by using a dual luciferase reporter assay system. Data are means ± SEM. Statistical analysis is based on one-way ANOVA followed by a Dunnett's test. $^{*}P < 0.05$, $^{**}P < 0.01$ *vs* untreated group or FFA treated group. (F) Hepa1-6 cells were pre-treated with 1 mM FFA for 12 h before Api treatment for 24 h. The indicated genes were measured by using qRT-PCR and normalized to β-actin levels. Data are means ± SEM. Statistical analysis is based on one-way ANOVA followed by a Dunnett's test. $^{*}P < 0.05$, $^{**}P < 0.01$ *vs* FFA treated group.

the Api-treated group and the vehicle control group (Fig. 4A), thus suggesting that Api did not affect Nrf2 mRNA expression. However, the Nrf2 protein level was significantly increased by Api in a dose-dependent manner (Fig. 4B) in the cell model, consistent with the results *in vivo* (Fig. 2F). Moreover, the level of Keap1 protein was also increased by Api treatment in the liver tissue compared with control group (Fig. 2F), which is agreed with Oscar Perez-Leal' study that Api as an inducer of Nrf2 was not independent of Keap1-mediated degradation. Interestingly, consistently with *in vivo* data, the nuclear Nrf2 level was decreased after FFA treatment but was clearly increased with increasing doses of Api. In contrast, the cytosolic increased Nrf2 was restored to control levels after Api treatment, thus suggesting that Api promoted Nrf2 translocation from cytoplasm to nucleus (Fig. 4C), which is also consistently with *in vivo* result (Fig. 2G). As expected, Nrf2 activity was significantly increased by Api assayed by luciferase reporter system (Fig. 4D). The mRNA levels of the lipid metabolism-related genes negatively regulated by Nrf2, which were notably up-regulated by FFA in the Hepa1-6 cells, were significantly down-regulated by Api (Fig. 4E). Meanwhile, the oxidative stress-

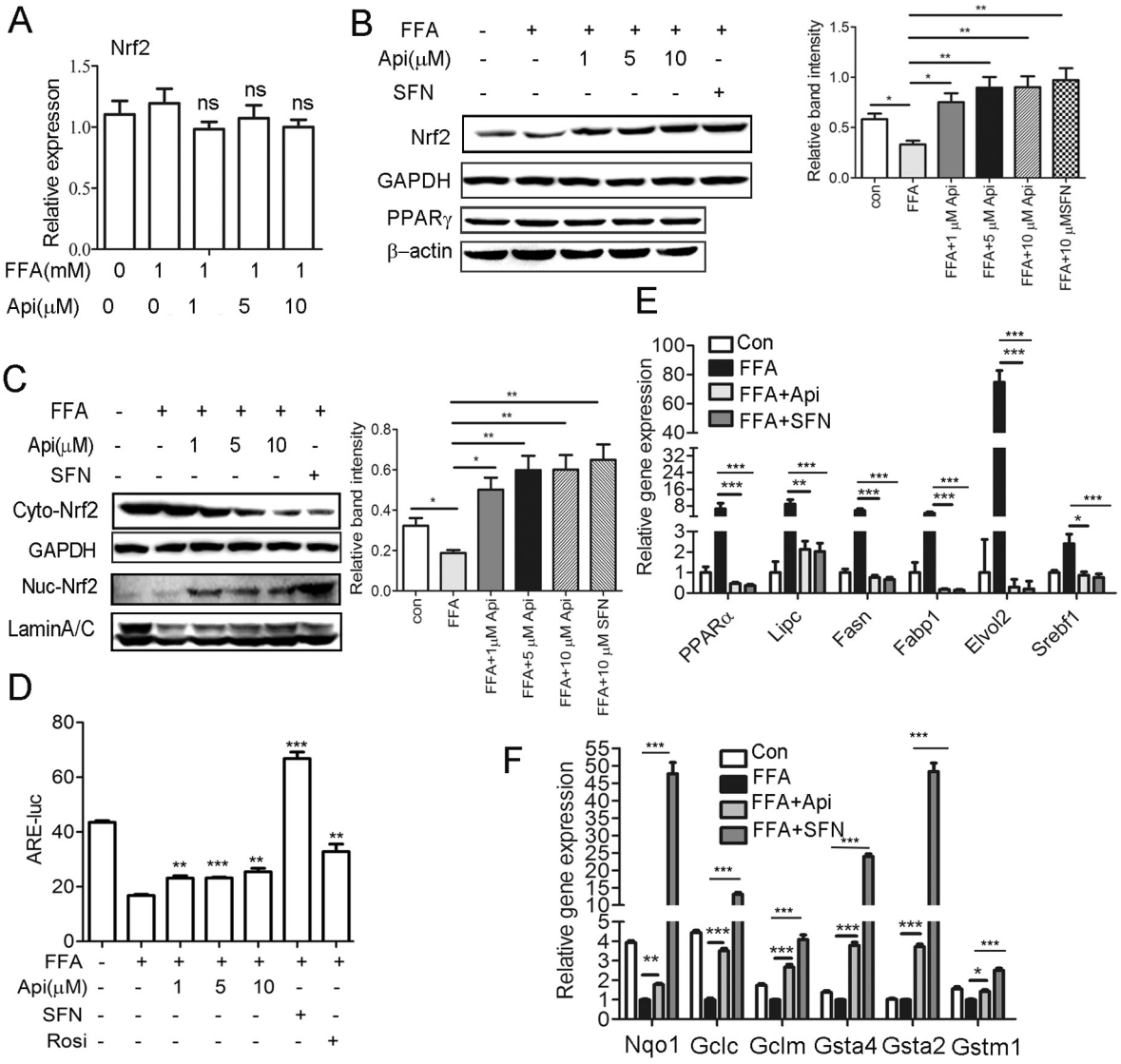

Fig. 4. Api regulates Nrf2 nucleocytoplasmic transport and activates Nrf2. (A) Hepa1-6 cells were pre-treated with 1 mM FFA for 12 h before Api treatment for 24 h. Nrf2 mRNA expression was measured by using qRT-PCR and normalized to β-actin levels. (B) The effect of Api on the expression of Nrf2, PPARγ proteins was detected by using western blotting and quantified by using Image J software. (C) Nuclear protein and cytoplasmic proteins were recovered from lysed Hepa1-6 cells treated with 1 mM FFA or 1 mM FFA plus different doses of Api, and were subjected to western blotting and quantified by using Image J software. (D) Transcriptional activation of Nrf2 in cells treated with 1 mM FFA or 1 mM FFA plus different doses of Api. Hep1-6 cells were transfected with plenti-mNrf2/ARE-Luc and pRL-control using Lipofectamine 2000. Then, cells were pre-treated with 1 mM FFA for 12 h before Api treatment for 24 h. The effect of Api on Nrf2 activity was evaluated by using a luciferase reporter system. (E) Relative mRNA expression of PPARα, Lipc, Fasn, Fabp1, Elvol2 and Srebf1 and (F) the oxidative stress-related genes, such as Nqo1, Gclc, Gclm, Gsta4, Gsta2 and Gstm1 were quantified by using qRT-PCR and normalized to β-actin levels. Data are means ± SEM. Statistical analysis is based on one-way ANOVA followed by a Dunnett's test. ns, not significant, $^{*}P < 0.05$, $^{**}P < 0.01$, $^{***}P < 0.001$ *vs* FFA treated group.

related genes, such as Nqo1, Gclc, Gclm, Gsta4, Gsta2 and Gstm1, which were clearly down-regulated by FFA in the Hepa1-6 cells, were significantly up-regulated by Api (Fig. 4F). Thus, Api can activate Nrf2, and thus regulating the corresponding genes targeted by Nrf2.

Additionally, in order to further examine the role of Nrf2 in Api induced inhibition of NAFLD progression, the expression of Nrf2 in hepatocytes was knocked down by specific shRNAs. At first, the efficacy of Nrf2 shRNA was verified by western blotting and qRT-PCR (Fig. 5A-B). When Nrf2 expression was inhibited by Nrf2 shRNA, the effects of Api on the mRNA levels of both lipid metabolism-related genes (PPARα, Lipc, Fasn, Fabp1, Elvol2, Srebf1 and Pla2g7) (Fig. 5C) and oxidative stress-related genes (Nqo1, Gclm, Gclc, Gsta4, Gsta2 and Gstm1) were abolished (Fig. 5D). Taken together, all these results suggest that the regulation of NAFLD progression by Api is dependent on Nrf2.

3.5. Api binds with Nrf2 to inhibit its function of activating PPARγ

According to our above results, the regulation of PPARγ target genes by Api might be associated with Nrf2 in hepatocytes. Firstly, Nrf2 was over-expressed in hepatocytes to detect the effect of Api on PPARγ activity. The data shown in Fig. 6A indicated that PPARγ activity was further inhibited after Nrf2 overexpressed, thus suggesting that Nrf2 negatively regulated PPARγ activity. Moreover, the expression of PPARγ downstream genes (Nrob2, Cidea, Fitm2, Fitm1 and G0s2) was further inhibited by Api in Nrf2 over-expressing cells (Fig. 6B). Additionally, PPARγ was significantly activated by Api after Nrf2 knock out by CRISPER/Cas9 system in NAFLD cell model (Fig. 6C). Certainly, after Nrf2 knockdown, the inhibition effect of Api on the mRNA levels of genes targeted by PPARγ were clearly eliminated (Fig. 6D). The same conclusion was obtained in Nrf2 knock out hepatocytes (Fig. 6E). These data

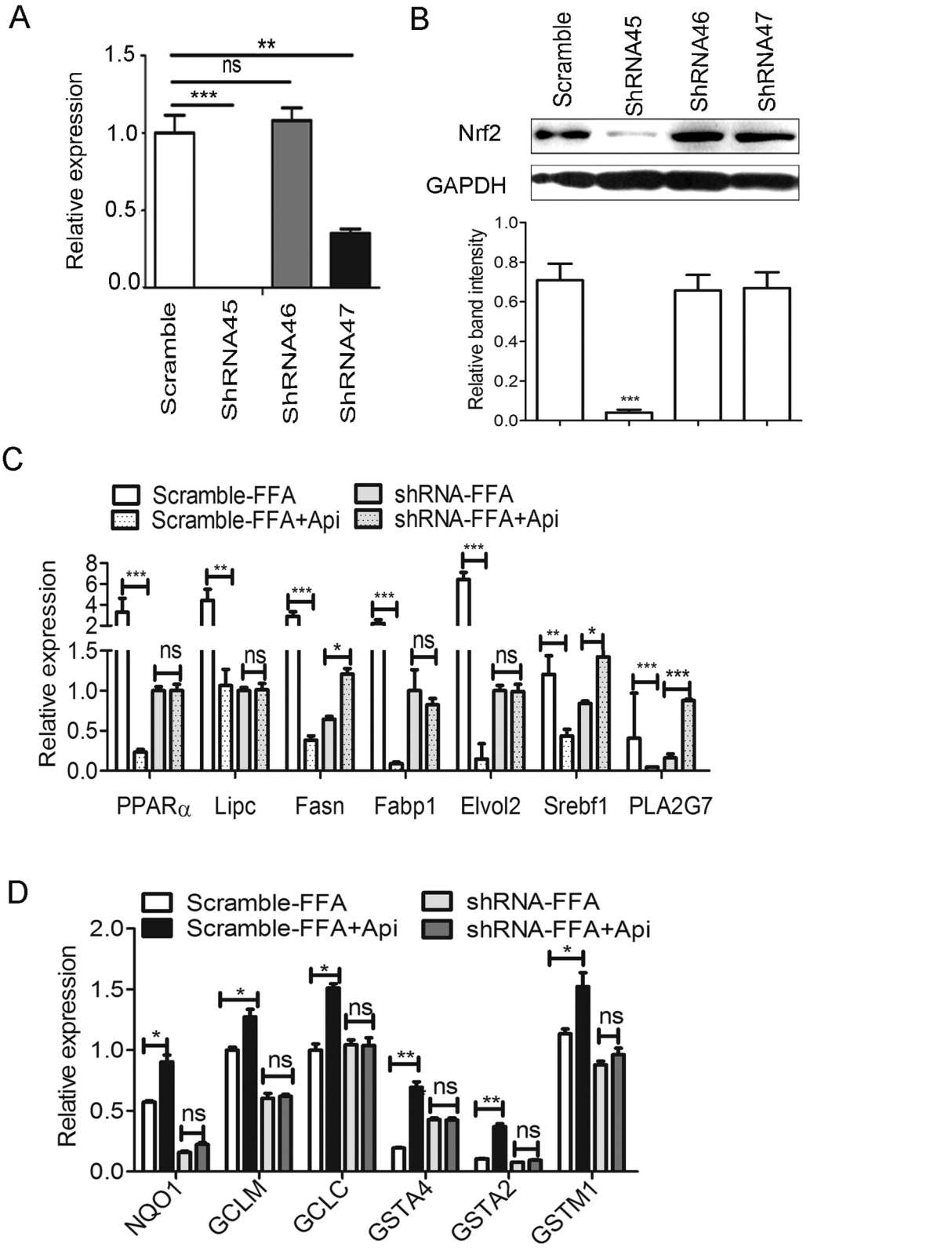

Fig.5. Nrf2 is necessary for Api inhibiting hepatocyte lipid metabolism disorder and oxidative stress induced by FFA *in vitro*. (A) Nrf2 mRNA level in Hepa1-6 cells transfected with scrambled or Nrf2 shRNA were evaluated by using qRT-PCR and normalized to β-actin levels. Data are means ± SEM. Statistical analysis is based on one-way ANOVA followed by a Dunnett's test. (B) Nrf2 protein expression level in Hepa1-6 cells transfected with scrambled or Nrf2 shRNA were evaluated by using western blotting and quantified by using Image J software. (C-D) Hep1-6 cells transfected with scrambled or Nrf2 shRNA were pre-treated with 1 mM FFA before Api treatment for 24 h, then subjected to qRT-PCR with the indicated probes (below graphs) and normalized to β-actin levels. Data are means ± SEM. All data shown are representative of three independent experiments. Statistical analysis is based on one-way ANOVA followed by a Dunnett's test. ns, not significant, $^{*}P < 0.05$, $^{**}P < 0.01$, $^{***}P < 0.001$ *vs* scramble-FFA or shRNA-FFA group.

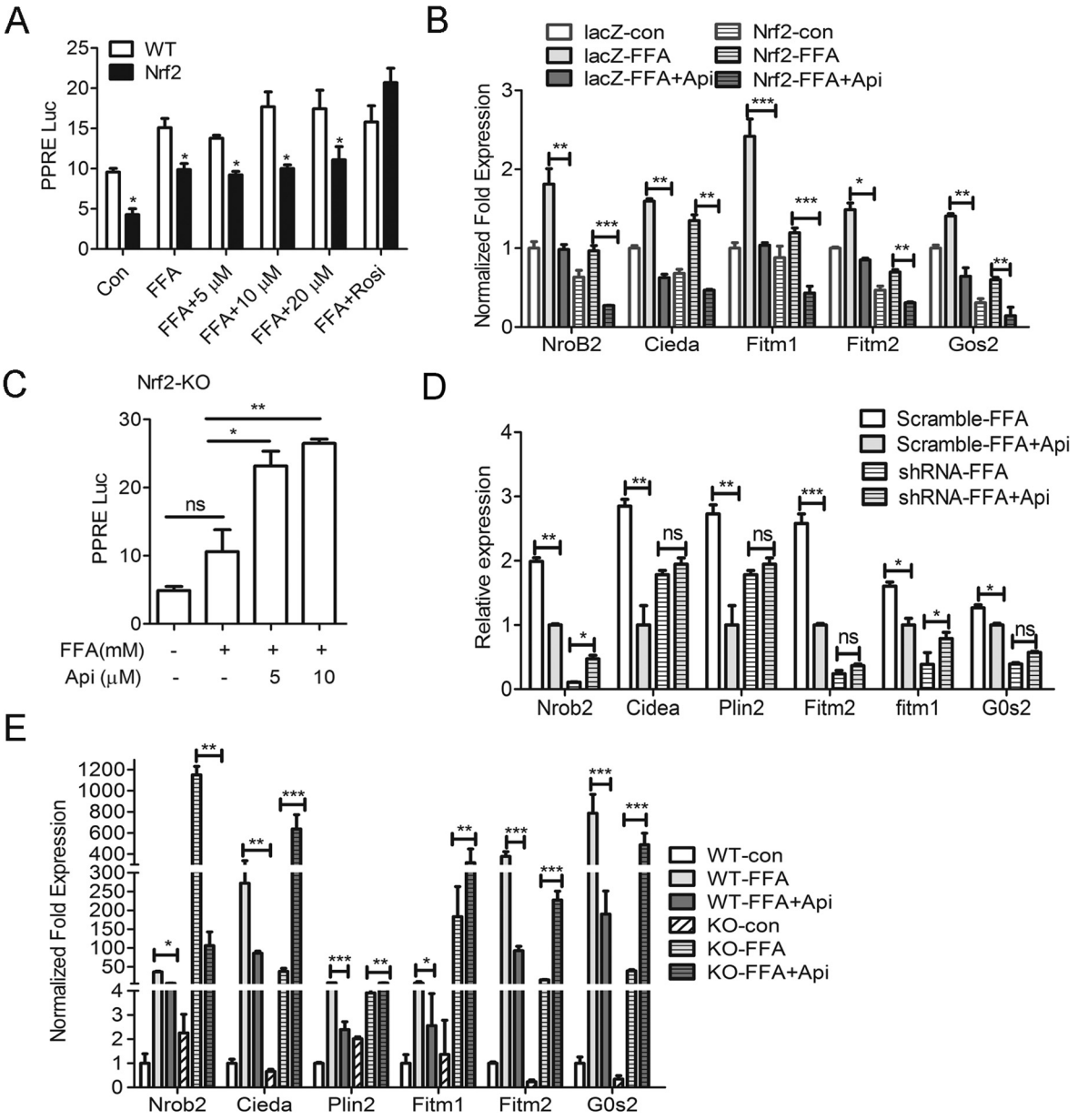

Fig. 6. Nrf2 negatively regulates PPARγ in the Api-treated NAFLD cell model. (A) Transcriptional activation of PPARγ in Nrf2 over-expression cells treated with FFA or FFA plus Api. Nrf2 over-expression cells were transfected with pIRES-mPPARγ/PPRE-Luc, pRL-control and PPARγ using Lipofectamine 2000. Then, cells were pre-treated with 1 mM FFA for 12 h before Api treatment for 24 h. Luciferase activity levels were measured by using a dual luciferase reporter assay system. (B) Hepa1-6 cells transfected with the lac-Z empty vector or Nrf2 vector were pre-treated with 1 mM FFA before Api treatment for 24 h, then subjected to qRT-PCR with the indicated probes (below graphs) and normalized to β-actin levels. Data are means ± SEM. Statistical analysis is based on one-way ANOVA followed by a Dunnett's test. $^{*}P < 0.05$, $^{**}P < 0.01$, $^{***}P < 0.001$ *vs* the lacZ-FFA or Nrf2-FFA group. (C) Transcriptional activation of PPARγ in Nrf2 knock out cells treated with FFA or FFA plus Api. Nrf2 knock out cells were transfected with pIRES-mPPARγ/PPRE-Luc, pRL-control and PPARγ using Lipofectamine 2000. Then, cells were pre-treated with 1 mM FFA for 12 h before Api treatment for 24 h. Luciferase activity levels were measured by using a dual luciferase reporter assay system. Data are means ± SEM. Statistical analysis is based on one-way ANOVA followed by a Dunnett's test. ns, not significant, $^{*}P < 0.05$, $^{**}P < 0.01$ *vs* the untreated group or FFA treated group. (D) Hepa1-6 cells transfected with scrambled empty vector or Nrf2 shRNA vector were pre-treated with 1 mM FFA before Api treatment for 24 h, followed by qRT-PCR with the indicated probes (below graphs) and normalized to β-actin levels. Data are means ± SEM. Statistical analysis is based on one-way ANOVA followed by a Dunnett's test. ns, not significant, $^{*}P < 0.05$, $^{**}P < 0.01$, $^{***}P < 0.001$ *vs* the scramble-FFA or ShRNA-FFA group. (E) Nrf2 knock out Hepa1-6 cells were pre-treated with 1 mM FFA before Api treatment for 24 h, followed by qRT-PCR with the indicated probes (below graphs) and normalized to β-actin levels. Data are means ± SEM. Statistical analysis is based on one-way ANOVA followed by a Dunnett's test. ns, not significant, $^{*}P < 0.05$, $^{**}P < 0.01$, $^{***}P < 0.001$ compared with the scramble-Api group. All data shown are representative of three independent experiments.

suggest that the activation effect of PPARγ is counteracted by Nrf2 activation by Api.

As we known, in macrophages and in lung of mice, Nrf2 regulated PPARγ expression by the interaction [47,48]. However, we did not detect the interaction between Nrf2 and PPARγ by using co-immunoprecipitation in hepatocytes (data not shown). Then we performed the molecular docking experiment to assay the interaction between Api and Nrf2 and the data shown in Fig. 7A indicated that the 4 and 7 hydroxyl hydrogen of Api could form H bonds with the residues of carboxyl oxygen of Nrf2's GLU496 or MET 499, separately. And the total binding free energy between Api and Nrf2 was −6.6 kcal/mol. Then, to explore whether Api can directly bind to Nrf2, we first expressed and purified the recombinant his6-tagged Nrf2 (Fig. 7B-C). Then qualitative method-ITC was employed to analyze the binding activity between Nrf2 and Api at 298 K. The binding affinity and binding stoichiometry of Nrf2 to

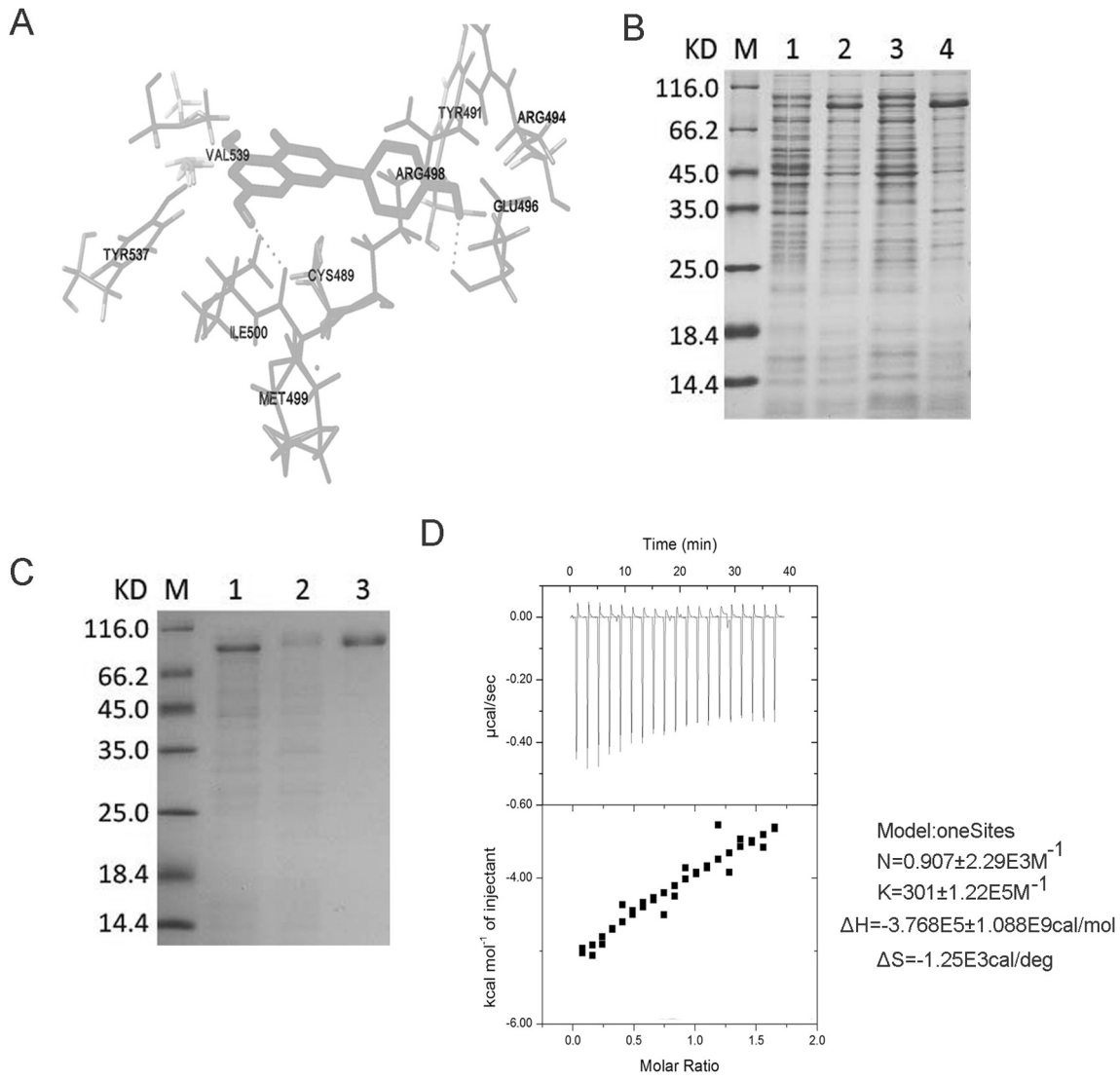

Fig. 7. Api binds with Nrf2. (A) Api can bind with Nrf2 at the sites of GLU496 and MET 499 via hydrogen bond. (B) The expression of Nrf2-his in bacteria was staining with coomassie brilliant blue. Lane M: Protein Marker, Lane 1: Un-induced, Lane 2: Induced, Lane3: supernatant of 11 degree induction with 0.5 mM IPTG, Lane 4: Precipitate of 11 degree induction with 0.5 mM IPTG. (C) The purification of Nrf2-his and the identification assay by using coomassie brilliant blue staining, Lane M: Protein marker, Lane 1: Un-purified, Lane 2: Flow through, Lane 3: Elution. (D) ITC data for binding of Api to Nrf2. The left panels show the raw data, and the right panels show the corresponding binding isotherm fitted according to the "one binding site" model. Reference titration of ligand into buffer was used to correct for heat of dilution. The thermodynamic parameters (K, ΔH, and ΔS) are indicated under the below.

Api were obtained via the one-site binding model fitting using integrated binding heat, which revealed 1 potential Api binding sites within Nrf2 with moderate binding affinity ($Ka = 301 \pm 1.22E5\ M^{-1}$) (Fig. 7D). Thus, we conclude that Api might binds with Nrf2 to inhibit its function of activating PPARγ, leading to the amelioration of NAFLD.

4. Discussion

NAFLD, the most common chronic liver disease strongly associated with obesity, is an emerging metabolic-related disorder characterized by fatty infiltration of the liver in the absence of alcohol consumption [49]. The disease ranges from simple steatosis to non-alcoholic steatohepatitis (NASH), includes a wide spectrum of liver disorders and markedly affects the health of affected individuals [50]. Currently, there is no approved pharmacological treatment for NAFLD although a large variety of phytochemicals and/or nutraceuticals have been concerned. A major challenge to drug therapies is that the detail mechanism remains elusive. Thus, studies on mechanisms of NAFLD and potential protective therapeutic interventions are important and topical.

PPARγ is a ligand-activated transcriptional factor [51] that has been recognized as the target of anti-diabetic drugs thiazolidinedione. Opinions differ regarding PPARγ activation in the liver. There have been concerns about the worsening of steatosis and liver injury when PPARγ ligands are administered to patients with NASH for de novo lipogenesis (DNL). Some studies have indicated that PPARγ activation induces novel, previously undefined mechanisms that attenuate NASH, including improved β-oxidation, which decreases hepatic steatosis, and the up-regulation of the Nrf2 pathway, which decreases oxidative stress, thereby overriding the PPARγ-induced DNL effects [29]. These opinions highlight the need for novel approaches, such as more selective PPARγ modulation, which can improve β-oxidation, decrease hepatic steatosis. Total flavonoids (TFs) from *Rosa laevigata* Michx fruit may serve as a new drug for NAFLD treatment [7]. Api, a widely distributed plant flavonoid, has been identified as a modulator of PPARγ that is effec-

tive in improving metabolic syndrome without the side effects of TZDs, by binding to different sites of PPARγ [15]. Here, we report that the pharmacological administration of Api effectively improves HFD-induced hepatic steatosis, hepatic lipid oxidation, lipogenesis and oxidative stress, thus suggesting that Api inhibits the progression of NAFLD. Although some previous reports have shown that increasing PPARγ expression is a feature of the steatotic liver and can activate lipogenic genes and DNL [52,53], it had no deleterious effects under conditions of HFD-induced hepatic steatosis and oxidative stress. In addition, the activation [29,54,55] of PPARγ by its ligands, can effectively attenuate NAFLD progression. However, the mechanism of PPARγ in modulating NAFLD is still elusive until now.

In our study, we found that the activities of anti-oxidant enzymes and lipid peroxidation were significantly restored by Api treatment. Interestingly, the activation function of PPARγ by Api disappeared in hepatocytes of NAFLD model but its target genes were markedly inhibited, suggesting there must be some negative regulatory factor of PPARγ involved in the event. As we know, transcription factor Nrf2 plays a central role in defense against oxidative stress and lipid metabolism abnormity [18,56]. In addition, cross-talk between PPARγ and Nrf2 has been well stated. Transfection of Nrf2 stimulates PPARγ promoter activity, and stable knockdown of Keap1 enhances PPARγ expression in 3T3-L1 cells [57]. Nrf2-induced PPARγ plays an essential protective role during the pathogenesis of pulmonary inflammation and oxidative stress in acute lung injury [47]. In contrast, Nrf2 can also be suppressed by activated PPARγ via a protein-protein interaction in macrophages [48]. In our study, we found that Nrf2 was translocated into the nucleus and the activity of Nrf2 was clearly increased by Api. The target genes of Nrf2, including anti-oxidant genes (Nqo1, Gclm, Gclc, Gsta4, Gsta2 and Gstm1) and lipid metabolic genes (PPARα, Lipc, Fasn, Fabp1, Elvol2 and Srebf1), were all expectedly affected by Api. Nrf2 knock down by specific shRNA or knock out by CRISPER/Cas9 system diminished the protective effects of Api on the oxidative stress and lipid metabolism of liver tissue. Meanwhile, Nrf2 overexpression enhanced the inhibition effect of Api on and the expression of the hepatocyte lipid metabolic genes. Thus, Nrf2 is required for Api ameliorating HFD-induced oxidative stress and lipid metabolic disorders of liver tissue.

Importantly, Nrf2 overexpression further inhibited the activity of PPARγ in the presence of Api. After Nrf2 knock out in hepatocytes, PPARγ activity was significantly activated by Api, indicating that the activation of Nrf2 by Api inhibited its function of activating PPARγ. As expected, the inhibition effects of PPARγ target genes induced by Api were blocked in Nrf2 knockdown cells. Together, the data indicated that Nrf2 activation induced novel mechanisms to decrease oxidative stress and override the PPARγ-induced DNL effects. For the mechanism, although we did not detect the interaction between Nrf2 and PPARγ (data not shown), the docking experiment indicated that Api can interact with Nrf2.

In summary, our findings demonstrated that Api had the efficacy on inhibiting NAFLD progression by improving the oxidative stress and the lipid metabolism abnormity of liver. Further mechanism study found that Api inhibited its function of activating PPARγ via Nrf2 activation. This study supplied a novel regulating mode of Nrf2 and PPARγ by Api in inhibiting lipid metabolism and oxidative stress abnormity to improve the progression of NAFLD and has potential importance in the field of NAFLD therapy.

Conflicts of interest

The authors declare that they have no competing interests.

Author contributions

F.X and S.P designed the experiments. F.X, Y.W, Z.F, L.X, S.Q and Z.W performed the experiments. F.X,Y.W and Z.F anayzed the data. F.X made the figures and wrote the manuscript. L.J provided critical commnents. Z.C and S.P supervised the project.

Acknowledgments

The work was supported by the open fund of State Key Laboratory of Pharmaceutical Biotechnology, Nanjing University, China (Grant No. KFGN-201501), and the National Natural Science Foundation of China (Nos. 81503082, 81673439 and 81473220), and the Natural Science Foundation of Jiangsu Province of China (No. BK20150575), and Postdoctoral Science Foundation of China (No. 2015M570437).

References

[1] P. Almeda-Valdes, D. Cuevas-Ramos, C.A. Aguilar-Salinas, Metabolic syndrome and non-alcoholic fatty liver disease, Ann. Hepatol. 8 (Suppl. 1) (2009) S18–S24.
[2] T. Karlas, J. Wiegand, T. Berg, Gastrointestinal complications of obesity: non-alcoholic fatty liver disease (NAFLD) and its sequelae, Best Pract. Res. Clin. Endocrinol. Metab. 27 (2) (2013) 195–208.
[3] Nonalcoholic fatty liver disease, Nat. Rev. Dis. Primers 1 (2015) 15081.
[4] B.W. Smith, L.A. Adams, Nonalcoholic fatty liver disease and diabetes mellitus: pathogenesis and treatment, Nat. Rev. Endocrinol. 7 (8) (2011) 456–465.
[5] M.E. Rinella, Nonalcoholic fatty liver disease: a systematic review, JAMA 313 (22) (2015) 2263–2273.
[6] B. Van De Wier, G.H. Koek, A. Bast, G.R. Haenen, The potential of flavonoids in the treatment of non-alcoholic fatty liver disease, Crit. Rev. Food Sci. Nutr. (2015).
[7] S. Zhang, L. Zheng, D. Dong, L. Xu, L. Yin, Y. Qi, X. Han, Y. Lin, K. Liu, J. Peng, Effects of flavonoids from Rosa laevigata Michx fruit against high-fat diet-induced non-alcoholic fatty liver disease in rats, Food Chem. 141 (3) (2013) 2108–2116.
[8] D. Arango, K. Morohashi, A. Yilmaz, K. Kuramochi, A. Parihar, B. Brahimaj, E. Grotewold, A.I. Doseff, Molecular basis for the action of a dietary flavonoid revealed by the comprehensive identification of apigenin human targets, Proc. Natl. Acad. Sci. U.S.A. 110 (24) (2013) E2153–E2162.
[9] J.M. Assini, E.E. Mulvihill, M.W. Huff, Citrus flavonoids and lipid metabolism, Curr. Opin. Lipidol. 24 (1) (2013) 34–40.
[10] Y.M. Yang, S.Y. Seo, T.H. Kim, S.G. Kim, Decrease of microRNA-122 causes hepatic insulin resistance by inducing protein tyrosine phosphatase 1B, which is reversed by licorice flavonoid, Hepatology 56 (6) (2012) 2209–2220.
[11] X. Zhai, M. Lin, F. Zhang, Y. Hu, X. Xu, Y. Li, K. Liu, X. Ma, X. Tian, J. Yao, Dietary flavonoid genistein induces Nrf2 and phase II detoxification gene expression via ERKs and PKC pathways and protects against oxidative stress in Caco-2 cells, Mol. Nutr. Food Res. 57 (2) (2013) 249–259.
[12] C.C. Buwa, U.B. Mahajan, C.R. Patil, S.N. Goyal, Apigenin attenuates beta-receptor-stimulated myocardial injury via safeguarding cardiac functions and escalation of antioxidant defence system, Cardiovasc. Toxicol. 16 (3) (2016) 286–297.
[13] X. Tong, J.C. Pelling, Targeting the PI3K/Akt/mTOR axis by apigenin for cancer prevention, Anticancer Agents Med. Chem. 13 (7) (2013) 971–978.
[14] S. Panda, A. Kar, Apigenin (4′,5,7-trihydroxyflavone) regulates hyperglycaemia, thyroid dysfunction and lipid peroxidation in alloxan-induced diabetic mice, J. Pharm. Pharmacol. 59 (11) (2007) 1543–1548.
[15] X. Feng, D. Weng, F. Zhou, Y.D. Owen, H. Qin, J. Zhao, WenYu, Y. Huang, J. Chen, H. Fu, N. Yang, D. Chen, J. Li, R. Tan, P. Shen, Activation of PPARgamma by a natural flavonoid modulator, apigenin ameliorates obesity-related inflammation via regulation of macrophage polarization, EBioMedicine (2016).
[16] A.M. Bataille, J.E. Manautou, Nrf2: a potential target for new therapeutics in liver disease, Clin. Pharmacol. Ther. 92 (3) (2012) 340–348.
[17] Y.K. Zhang, R.L. Yeager, Y. Tanaka, C.D. Klaassen, Enhanced expression of Nrf2 in mice attenuates the fatty liver produced by a methionine- and choline-deficient diet, Toxicol. Appl. Pharmacol. 245 (3) (2010) 326–334.
[18] Y. Tanaka, L.M. Aleksunes, R.L. Yeager, M.A. Gyamfi, N. Esterly, G.L. Guo, C.D. Klaassen, NF-E2-related factor 2 inhibits lipid accumulation and oxidative stress in mice fed a high-fat diet, J. Pharmacol. Exp. Ther. 325 (2) (2008) 655–664.
[19] K. Itoh, J. Mimura, M. Yamamoto, Discovery of the negative regulator of Nrf2, Keap1: a historical overview, Antioxid. Redox Signal. 13 (11) (2010) 1665–1678.
[20] J. Lamle, S. Marhenke, J. Borlak, R. von Wasielewski, C.J. Eriksson, R. Geffers, M. P. Manns, M. Yamamoto, A. Vogel, Nuclear factor-erythroid 2-related factor 2 prevents alcohol-induced fulminant liver injury, Gastroenterology 134 (4) (2008) 1159–1168.

[21] X. Paredes-Gonzalez, F. Fuentes, Z.Y. Su, A.N. Kong, Apigenin reactivates Nrf2 anti-oxidative stress signaling in mouse skin epidermal JB6 P + cells through epigenetics modifications, AAPS J. 16 (4) (2014) 727–735.
[22] X. Paredes-Gonzalez, F. Fuentes, S. Jeffery, C.L. Saw, L. Shu, Z.Y. Su, A.N. Kong, Induction of NRF2-mediated gene expression by dietary phytochemical flavones apigenin and luteolin, Biopharm. Drug Dispos. 36 (7) (2015) 440–451.
[23] M.V. Machado, G.A. Michelotti, G. Xie, T. Almeida Pereira, J. Boursier, B. Bohnic, C.D. Guy, A.M. Diehl, Mouse models of diet-induced nonalcoholic steatohepatitis reproduce the heterogeneity of the human disease, PLoS ONE 10 (5) (2015) e0127991.
[24] A. Tailleux, K. Wouters, B. Staels, Roles of PPARs in NAFLD: potential therapeutic targets, Biochim. Biophys. Acta 1821 (5) (2012) 809–818.
[25] E. Moran-Salvador, M. Lopez-Parra, V. Garcia-Alonso, E. Titos, M. Martinez-Clemente, A. Gonzalez-Periz, C. Lopez-Vicario, Y. Barak, V. Arroyo, J. Claria, Role for PPARgamma in obesity-induced hepatic steatosis as determined by hepatocyte- and macrophage-specific conditional knockouts, FASEB J. 25 (8) (2011) 2538–2550.
[26] T. Yamazaki, S. Shiraishi, K. Kishimoto, S. Miura, O. Ezaki, An increase in liver PPARgamma2 is an initial event to induce fatty liver in response to a diet high in butter: PPARgamma2 knockdown improves fatty liver induced by high-saturated fat, J. Nutr. Biochem. 22 (6) (2011) 543–553.
[27] I. Garcia-Ruiz, C. Rodriguez-Juan, T. Diaz-Sanjuan, M.A. Martinez, T. Munoz-Yague, J.A. Solis-Herruzo, Effects of rosiglitazone on the liver histology and mitochondrial function in ob/ob mice, Hepatology 46 (2) (2007) 414–423.
[28] M. Peyrou, P. Ramadori, L. Bourgoin, M. Foti, PPARs in liver diseases and cancer: epigenetic regulation by microRNAs, PPAR Res. 2012 (2012) 757803.
[29] A.A. Gupte, J.Z. Liu, Y. Ren, L.J. Minze, J.R. Wiles, A.R. Collins, C.J. Lyon, D. Pratico, M.J. Finegold, S.T. Wong, P. Webb, J.D. Baxter, D.D. Moore, W.A. Hsueh, Rosiglitazone attenuates age- and diet-associated nonalcoholic steatohepatitis in male low-density lipoprotein receptor knockout mice, Hepatology 52 (6) (2010) 2001–2011.
[30] N.K. Salam, T.H. Huang, B.P. Kota, M.S. Kim, Y. Li, D.E. Hibbs, Novel PPAR-gamma agonists identified from a natural product library: a virtual screening, induced-fit docking and biological assay study, Chem. Biol. Drug Des. 71 (1) (2008) 57–70.
[31] M. Mueller, B. Lukas, J. Novak, T. Simoncini, A.R. Genazzani, A. Jungbauer, Oregano: a source for peroxisome proliferator-activated receptor gamma antagonists, J. Agric. Food Chem. 56 (24) (2008) 11621–11630.
[32] A.E. Feldstein, N.W. Werneburg, A. Canbay, M.E. Guicciardi, S.F. Bronk, R. Rydzewski, L.J. Burgart, G.J. Gores, Free fatty acids promote hepatic lipotoxicity by stimulating TNF-alpha expression via a lysosomal pathway, Hepatology 40 (1) (2004) 185–194.
[33] D. Shi, X. Zhan, X. Yu, M. Jia, Y. Zhang, J. Yao, X. Hu, Z. Bao, Inhibiting CB1 receptors improves lipogenesis in an in vitro non-alcoholic fatty liver disease model, Lipids Health Dis. 13 (2014) 173.
[34] O. Shalem, N.E. Sanjana, E. Hartenian, X. Shi, D.A. Scott, T.S. Mikkelsen, D. Heckl, B.L. Ebert, D.E. Root, J.G. Doench, F. Zhang, Genome-scale CRISPR-Cas9 knockout screening in human cells, Science 343 (6166) (2014) 84–87.
[35] K.J. Livak, T.D. Schmittgen, Analysis of relative gene expression data using real-time quantitative PCR and the 2(−Delta Delta C(T)) Method, Methods 25 (4) (2001) 402–408.
[36] X. Feng, D. Weng, F. Zhou, Y.D. Owen, H. Qin, J. Zhao, WenYu, Y. Huang, J. Chen, H. Fu, N. Yang, D. Chen, J. Li, R. Tan, P. Shen, Activation of PPARgamma by a natural flavonoid modulator, apigenin ameliorates obesity-related inflammation via regulation of macrophage polarization, EBioMedicine 9 (2016) 61–76.
[37] I.A. Kirpich, L.N. Gobejishvili, M. Bon Homme, S. Waigel, M. Cave, G. Arteel, S.S. Barve, C.J. McClain, I.V. Deaciuc, Integrated hepatic transcriptome and proteome analysis of mice with high-fat diet-induced nonalcoholic fatty liver disease, J. Nutr. Biochem. 22 (1) (2011) 38–45.
[38] A.H. Mokdad, E.S. Ford, B.A. Bowman, W.H. Dietz, F. Vinicor, V.S. Bales, J.S. Marks, Prevalence of obesity, diabetes, and obesity-related health risk factors, 2001, JAMA 289 (1) (2003) 76–79.
[39] M.A. Abdelmegeed, S.H. Yoo, L.E. Henderson, F.J. Gonzalez, K.J. Woodcroft, B.J. Song, PPARalpha expression protects male mice from high fat-induced nonalcoholic fatty liver, J. Nutr. 141 (4) (2011) 603–610.
[40] C.P. Day, O.F. James, Steatohepatitis: a tale of two "hits"? Gastroenterology 114 (4) (1998) 842–845.
[41] G. Colombo, M. Clerici, M.E. Garavaglia, D. Giustarini, R. Rossi, A. Milzani, I. Dalle-Donne, A step-by-step protocol for assaying protein carbonylation in biological samples, J. Chromatogr. B Analyt. Technol. Biomed. Life Sci. (2015).
[42] N.R. Kitteringham, A. Abdullah, J. Walsh, L. Randle, R.E. Jenkins, R. Sison, C.E. Goldring, H. Powell, C. Sanderson, S. Williams, L. Higgins, M. Yamamoto, J. Hayes, B.K. Park, Proteomic analysis of Nrf2 deficient transgenic mice reveals cellular defence and lipid metabolism as primary Nrf2-dependent pathways in the liver, J. Proteomics 73 (8) (2010) 1612–1631.
[43] C. Yan, W. Sun, X. Wang, J. Long, X. Liu, Z. Feng, J. Liu, Punicalagin attenuates palmitate-induced lipotoxicity in HepG2 cells by activating the Keap1-Nrf2 antioxidant defense system, Mol. Nutr. Food Res. (2016).
[44] J. Du, M. Zhang, J. Lu, X. Zhang, Q. Xiong, Y. Xu, Y. Bao, W. Jia, Osteocalcin improves nonalcoholic fatty liver disease in mice through activation of Nrf2 and inhibition of JNK, Endocrine (2016).
[45] S. Hatia, A. Septembre-Malaterre, F. Le Sage, A. Badiou-Beneteau, P. Baret, B. Payet, C. Lefebvre d'hellencourt, M.P. Gonthier, Evaluation of antioxidant properties of major dietary polyphenols and their protective effect on 3T3-L1 preadipocytes and red blood cells exposed to oxidative stress, Free Radic. Res. 48 (4) (2014) 387–401.
[46] X. Paredes-Gonzalez, F. Fuentes, Z.Y. Su, A.N.T. Kong, Apigenin reactivates Nrf2 anti-oxidative stress signaling in mouse skin epidermal JB6 P + cells through epigenetics modifications, Aaps J. 16 (4) (2014) 727–735.
[47] H.Y. Cho, W. Gladwell, X. Wang, B. Chorley, D. Bell, S.P. Reddy, S.R. Kleeberger, Nrf2-regulated PPAR{gamma} expression is critical to protection against acute lung injury in mice, Am. J. Respir. Crit. Care Med. 182 (2) (2010) 170–182.
[48] Y. Ikeda, A. Sugawara, Y. Taniyama, A. Uruno, K. Igarashi, S. Arima, S. Ito, K. Takeuchi, Suppression of rat thromboxane synthase gene transcription by peroxisome proliferator-activated receptor gamma in macrophages via an interaction with NRF2, J. Biol. Chem. 275 (42) (2000) 33142–33150.
[49] A. Ahmed, R.J. Wong, S.A. Harrison, Nonalcoholic fatty liver disease review: diagnosis, treatment, and outcomes, Clin. Gastroenterol. Hepatol. 13 (12) (2015) 2062–2070.
[50] G. Marchesini, E. Bugianesi, G. Forlani, F. Cerrelli, M. Lenzi, R. Manini, S. Natale, E. Vanni, N. Villanova, N. Melchionda, M. Rizzetto, Nonalcoholic fatty liver, steatohepatitis, and the metabolic syndrome, Hepatology 37 (4) (2003) 917–923.
[51] J.M. Lehmann, L.B. Moore, T.A. Smith-Oliver, W.O. Wilkison, T.M. Willson, S.A. Kliewer, An antidiabetic thiazolidinedione is a high affinity ligand for peroxisome proliferator-activated receptor gamma (PPAR gamma), J. Biol. Chem. 270 (22) (1995) 12953–12956.
[52] S. Yu, K. Matsusue, P. Kashireddy, W.Q. Cao, V. Yeldandi, A.V. Yeldandi, M.S. Rao, F.J. Gonzalez, J.K. Reddy, Adipocyte-specific gene expression and adipogenic steatosis in the mouse liver due to peroxisome proliferator-activated receptor gamma1 (PPARgamma1) overexpression, J. Biol. Chem. 278 (1) (2003) 498–505.
[53] O. Gavrilova, M. Haluzik, K. Matsusue, J.J. Cutson, L. Johnson, K.R. Dietz, C.J. Nicol, C. Vinson, F.J. Gonzalez, M.L. Reitman, Liver peroxisome proliferator-activated receptor gamma contributes to hepatic steatosis, triglyceride clearance, and regulation of body fat mass, J. Biol. Chem. 278 (36) (2003) 34268–34276.
[54] A. Galli, D.W. Crabb, E. Ceni, R. Salzano, T. Mello, G. Svegliati-Baroni, F. Ridolfi, L. Trozzi, C. Surrenti, A. Casini, Antidiabetic thiazolidinediones inhibit collagen synthesis and hepatic stellate cell activation in vivo and in vitro, Gastroenterology 122 (7) (2002) 1924–1940.
[55] L. Yang, S.A. Stimpson, L. Chen, W. Wallace Harrington, D.C. Rockey, Effectiveness of the PPARgamma agonist, GW570, in liver fibrosis, Inflamm. Res. 59 (12) (2010) 1061–1071.
[56] S. Shin, J. Wakabayashi, M.S. Yates, N. Wakabayashi, P.M. Dolan, S. Aja, K.T. Liby, M.B. Sporn, M. Yamamoto, T.W. Kensler, Role of Nrf2 in prevention of high-fat diet-induced obesity by synthetic triterpenoid CDDO-imidazolide, Eur. J. Pharmacol. 620 (1–3) (2009) 138–144.
[57] J. Pi, L. Leung, P. Xue, W. Wang, Y. Hou, D. Liu, E. Yehuda-Shnaidman, C. Lee, J. Lau, T.W. Kurtz, J.Y. Chan, Deficiency in the nuclear factor E2-related factor-2 transcription factor results in impaired adipogenesis and protects against diet-induced obesity, J. Biol. Chem. 285 (12) (2010) 9292–9300.